Molecular Biology of the Cell
Vol. 15, 2436–2448, May 2004

Identification of Novel Principles of Keratin Filament Network Turnover in Living Cells[V]

Reinhard Windoffer, Stefan Wöll, Pavel Strnad, and Rudolf E. Leube*

Department of Anatomy, Johannes Gutenberg University, 55128 Mainz, Germany

Submitted September 30, 2003; Revised January 22, 2004; Accepted January 22, 2004
Monitoring Editor: Paul Matsudaira

It is generally assumed that turnover of the keratin filament system occurs by exchange of subunits along its entire length throughout the cytoplasm. We now present evidence that a circumscribed submembranous compartment is actually the main site for network replenishment. This conclusion is based on the following observations in living cells synthesizing fluorescent keratin polypeptides: 1) Small keratin granules originate in close proximity to the plasma membrane and move toward the cell center in a continuous motion while elongating into flexible rod-like fragments that fuse with each other and integrate into the peripheral KF network. 2) Recurrence of fluorescence after photobleaching is first seen in the cell periphery where keratin filaments are born that translocate subsequently as part of the network toward the cell center. 3) Partial keratin network reformation after orthovanadate-induced disruption is restricted to a distinct peripheral zone in which either keratin granules or keratin filaments are transiently formed. These findings extend earlier investigations of mitotic cells in which de novo keratin network formation was shown to originate from the cell cortex. Taken together, our results demonstrate that the keratin filament system is not homogenous but is organized into temporally and spatially distinct subdomains. Furthermore, the cortical localization of the regulatory cues for keratin filament turnover provides an ideal way to adjust the epithelial cytoskeleton to dynamic cellular processes.

INTRODUCTION

The cytoskeleton is a main structural feature of eukaryotic cells determining cell shape and facilitating a variety of cell functions. It consists of extensive, interconnected three-dimensional (3D) networks that are composed of microtubules, microfilaments, and intermediate filaments (IFs). Within epithelial cells, the abundant IFs are typically composed of keratin polypeptides. Keratin filaments (KFs) are connected to desmosomal cell-cell contact sites and to hemidesmosomal cell-substratum contacts, thereby forming a well-anchored supracellular scaffolding that is the major stabilizing element of multilayered epithelial tissues (recent reviews in Coulombe and Omary, 2002; Herrmann *et al.*, 2003). Despite the undisputed stabilizing properties of KF networks, they must be highly flexible and dynamic to facilitate adaptation to processes that require deformation of either the entire cell or certain parts thereof. Such cytoskeletal modulation is needed physiologically during cell division, migration, or differentiation and is also a prerequisite for metastasis of malignant cells.

A fundamental difference between the three cytoskeletal networks is the polarity of the actin and microtubule systems, whereas IFs are intrinsically nonpolar as a result of the antiparallel arrangement of dimers within their tetrameric building blocks (Parry and Steinert, 1999; Strelkov *et al.*, 2003). Therefore, a homogenous, nondifferential IF organization has been proposed that is supported by experiments in which incorporation of IF polypeptides was noted at multiple sites within the entire filament network without topological preference (Kreis *et al.*, 1983; Vikstrom *et al.*, 1989; Ngai *et al.*, 1990; Miller *et al.*, 1991, 1993; Coleman and Lazarides, 1992). In this way, the principally endless filament system could be maintained by continuous lateral exchange of subunits with the soluble keratin pool without disruption of network integrity. Support for this model was found in fluorescence recovery after photobleaching (FRAP) experiments of cells synthesizing fluorescently labeled IFs, in which gradual recurrence of fluorescence was observed in bleached zones of filaments (Vikstrom *et al.*, 1992; Yoon *et al.*, 1998, 2001). Furthermore, transient treatment of cells with the tyrosine phosphatase inhibitor orthovanadate led to formation of keratin granules at multiple cytoplasmic sites that directly retransformed in loco into filaments after drug removal (Strnad *et al.*, 2002). The multifocal exchange mechanism, however, has several unresolved questions: e.g., how do filaments multiply, how is filament diameter and length regulated, and how are filaments formed de novo. In addition, the regulation of localized IF network alteration would be difficult to envision given the principle equivalence of all filaments.

Alternatively, IF organizing centers have been proposed to exist in various cellular subdomains such as adhesion sites (Knapp *et al.*, 1983; Bologna *et al.*, 1986), certain plasma membrane domains (Georgatos and Blobel, 1987; Georgatos *et al.*, 1987), the nucleus (Eckert *et al.*, 1982; Albers and Fuchs, 1987; Georgatos and Blobel, 1987; Georgatos *et al.*, 1987), or cytoplasmic sites (Kreis *et al.*, 1983; Celis *et al.*, 1984; Magin *et al.*, 1990; Raats *et al.*, 1990; Sarria *et al.*, 1990). These centers might function both as initiation sites for KF formation and as regions from which KF turnover is regulated. The nonconclusive nature of the reported observations so far and the

Article published online ahead of print. Mol. Biol. Cell 10.1091/mbc.E03–09–0707. Article and publication date are available at www.molbiolcell.org/cgi/doi/10.1091/mbc.E03–09–0707.

[V] Online version of this article contains supporting material. Online version is available at www.molbiolcell.org.

* Corresponding author. E-mail address: leube@uni-mainz.de.

Abbreviations used: FRAP, fluorescence recovery after photobleaching; IF, intermediate filament; KF, keratin filament; PBS, phosphate-buffered saline; ULF, unit length filament.

contradictory results, however, have been impediments to universally accepted concepts for spatially defined KF network turnover and formation. We have recently proposed that the actin-rich subplasmalemmal domain, the cell cortex, may serve as an organizing region from which network formation originates at the end of mitosis (Windoffer and Leube, 2001). This proposal was based on monitoring fluorescent keratins in dividing epithelial A-431 cells that completely disassembled their KF network into soluble material and granular aggregates and reformed their network exclusively from the cell periphery.

In the present study we provide further evidence for the second model of spatially defined keratin organization showing that continuous de novo formation of keratins in the cell periphery is a general principle in epithelial cells and that KF turnover is a multistep process originating primarily from the cell cortex. These mechanisms are ideally suited to adapt the KF cytoskeleton to varying cellular requirements.

MATERIALS AND METHODS

DNA Cloning

To construct a cDNA coding for a fluorescent K8 hybrid, we amplified a 3′-fragment from the previously described human K8 cDNA (Hofmann and Franke, 1997) by PCR using amplimers 00-01 5′-CGG CTA TGC AGG TGG TCT GAG-3′ and 00-02 5′-AAA GGA TCC TTG GGC AGG ACG TCA GAG GA-3′. The *Sac*I-*Bam*HI–cleaved PCR product was cloned together with the *Eco*RI-*Sac*I–limited K8 cDNA 5′-fragment in pECFP-N1 (Clontech Laboratories, Palo Alto, CA). The resulting cDNA codes for fusion protein HK8-CFP consisting of the entire human K8 with enhanced cyan fluorescent protein at its carboxyterminus. Both polypeptides are connected by the short linker sequence DPPVAT. A cDNA coding for HK18-YFP has been described previously (Strnad *et al.*, 2002).

Human K5 and K14 cDNAs were generously provided by Dr. Harald Herrmann (German Cancer Research Centre, Heidelberg, Germany) and were used as templates for PCR with either primers 00-50 5′-AAA AAG CTT ATG TCT CGC CAG TCA AGT GTG-3′ and 00-51 5′-AAA GGA TCC GGG CTC TTG AAG CTC TTC CGG GA-3′ for K5 or primers 00-52 5′-AAA AAG CTT ATG ACT ACC TGC AGC CGC CAG-3′ and 00-53 5′-AAA GGA TCC GGG TTC TTG GTG CGA AGG ACC TG-3′ for K14. The amplified fragments were digested with *Hin*dIII/*Bam*HI and inserted into either pECFP-N1 for K5 (encoded fusion protein HK5-CFP) or pEYFP-N1 (Clontech Laboratories) for K14 (corresponding fusion protein HK14-YFP). A cDNA coding for EYFP-K14 was kindly provided by Dr. Nicola Werner (Department of Biochemistry, Bonn University, Germany).

Cell Lines and cDNA Transfection

The following cell lines were used and cultured according to the specifications given by ATCC or the respective references: rat kangaroo kidney PtK2 cells (ATCC CCL-56), Madin-Darby canine kidney (MDCK) cells (clone 20; ATCC CCL-34), bovine kidney-derived MDBK cells (ATCC CCL-22), human mammary adenocarcinoma-derived MCF7 cells (ATCC HTB-22), human hepatocellular carcinoma-derived PLC cells (ATCC CRL8024), human colon carcinoma CaCo-2 cells (ATCC HTB-37), human immortalized HaCaT keratinocytes (Boukamp *et al.*, 1988), and human small-cell carcinoma SW13 cells derived from the adrenal cortex (ATCC CCL-105). Primary murine keratinocytes were prepared from trunks of newborn C57/BL6J mice and maintained exactly as described (Hager *et al.*, 1999). Primary human keratinocytes were obtained from Invitrogen GmbH (Karlsruhe, Germany) and were passaged according to the recommendations provided by the distributor. In addition, the following stably transfected cell lines were used: AK13–1 producing HK13-EGFP (Windoffer and Leube, 1999), PK18–5 synthesizing HK18-YFP (Strnad *et al.*, 2002), and A-431 clone B5 expressing CoDg-cDNA (Troyanovsky *et al.*, 1993).

Transient and stable transfections using the calcium phosphate precipitation method were done essentially as described previously (Leube *et al.*, 1989). Alternatively, the GenePORTER 2 transfection reagent was used for lipofection (from PEQLAB Biotechnologie GmbH, Erlangen, Germany). To this end, 10 μl serum-free medium was mixed with 10 μl hydrated GenePORTER 2 reagent and was added to 2 μg DNA freshly diluted to 50 μl with the provided diluent B. The resulting solution was incubated for 10 min at room temperature and added dropwise to subconfluent cells in 2-cm-diameter Petri dishes. After overnight incubation the medium was changed. Cells were analyzed after 24–48 h.

Life Cell Imaging

For time-lapse fluorescence microscopy of living cells, phenol-red–free Hanks' medium (Invitrogen GmbH) was used. Images were recorded by epifluorescence microscopy using inverse optics (Olympus, Hamburg, Germany) and an attached IMAGO slow-scan CCD camera (TILL Photonics, Gräfelfing, Germany) as described previously (Windoffer *et al.*, 2002). The microscope was kept in a climate chamber at 37°C with the cells grown in a Petri dish with a glass bottom (Mattek, Ashland, MA). In some instances, sodium orthovanadate (Aldrich, Milwaukee, WI) was added to the medium. The whole system was controlled by TILLvisION software (TILL Photonics). Excitation with monochromatic light of 496 nm was accomplished with a monochromator. Alternatively, living cells were recorded with a confocal laser scan microscope (Leica TCS SP2; Leica Microsystems, Bensheim, Germany) using an argon laser (λ = 488 nm). The emitted light was monitored between 500 and 590 nm. Images were imported into Image-ProPlus 4.5 (MediaCybernetics, Silver Spring, MD) and converted into movies (QuickTime 5.0, Apple, Cupertino, CA). The position of cell borders was determined from transmitted light images that were recorded in parallel. Amira software (TGS Europe, Merignac, France) was used to generate 3D reconstructions of confocal stacks using either the surface or the voltex presentation.

Fluorescence Recovery after Photobleaching

FRAP experiments were carried out with a Leica TCS SP2 confocal microscope. The 488-nm line of an argon/krypton laser was used for both bleaching and image recording. The emitted light was monitored between 500 and 590 nm. Recordings were performed via a 63× 1.4 NA oil immersion objective. Standard settings for prebleach and recovery image scans were 6% of minimum laser power, a line average of 4 and a gain of 800. A wide pinhole size (setting of 500) was chosen for high depth of focus, minimal photobleaching, and a strong fluorescence signal. Bleaching in the chosen areas of interest was carried out at 100% of medium laser power for a total of 20 scans. Bleaching of large areas was achieved by successive bleaching of subregions. Under these conditions, bleaching was practically complete not only in the focal recording plane but also in the regions above and below, thereby excluding the possibility that focal shift or cell motility could recover new sources of fluorescent material. The microscope was set to prebleach parameters immediately after bleaching, and images were recorded at regular intervals. Transmitted light images were recorded simultaneously to assess viability of cells.

Diagrams

The following different types of diagram were prepared from life cell images to highlight various aspects of dynamic keratin behavior.

Mobility Diagrams. To this end a line was selected from fluorescence recordings, that was rectangular to the cell edge and extended from outside the cell toward the cell center. Amira software was used to depict the fluorescence distribution along this line during time.

Time-space Diagrams. In this instance, distinct structures were cut out from successive recordings and the resulting pictures were imported into Amira. From these image data trajectories were derived that presented the surface view of the structures in time and space.

Diagrams of Reappearing Fluorescence in Relation to Time and Intracellular Topology. For FRAP experiments, the 12-bit gray values of selected areas were quantified using Image-ProPlus (Media Cybernetics, Göttingen, Germany) and analyzed using Excel spreadsheet routines (Microsoft, Redmond, WA). In some instances, fluorescence intensity was measured along a single line. The alterations of the gray levels were then plotted as a surface view with color-coded intensity peaks during time with the help of Amira software.

Diagrams of Growth Kinetics of Individual Particles. Individual KF precursors were selected by hand and cut out in consecutive micrographs, resulting in image sequences that depicted the growth of the particles and their alterations over time. The length and width of the precursors was analyzed with Image-ProPlus at each time point, using both, the longest caliper (feret max) and the shortest caliper (feret min) measurement. A total of 10 particles occurring in different cells were measured in this way and the resulting measurements were plotted vs. time.

RESULTS

Continuous Centripetal Keratin Movement Is a Common Property of Diverse Epithelial Cell Types and Nonepithelial Cells

To study the dynamic behavior of KFs, we have established cell lines that synthesize fluorescent human keratin chimeras (Windoffer and Leube, 1999; Strnad *et al.*, 2002). We have shown that these hybrid polypeptides integrate into fully

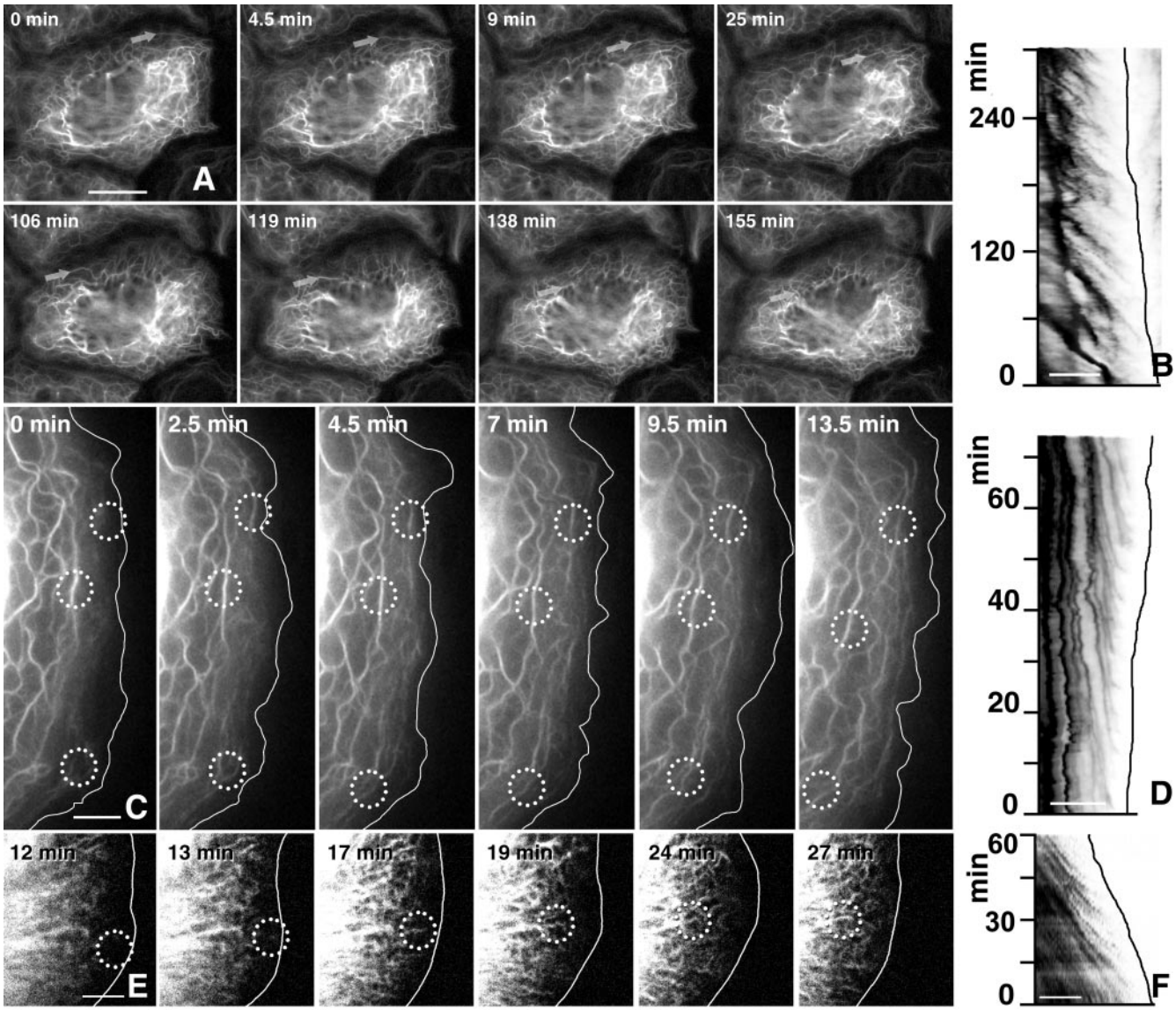

Figure 1. Detection of keratin dynamics by epifluorescence microscopy in living hepatocellular carcinoma–derived PK18–5 cells synthesizing fluorescent keratin chimeras HK18-YFP (A–D) and in a primary human keratinocyte producing fluorescent HK14-YFP chimeras (E and F) either by epifluorescence microscopy (A–D) or by confocal laser scanning microscopy (E and F). (A, C, and E) Fluorescence micrographs taken from movies 1–3, respectively, depict the alterations of the keratin system in a confluent monolayer at low magnification (A) and at free cell borders at high magnification (C and E; position of plasma membrane demarcated by white line). Note the similarity of the overall KF network organization throughout the observation period in each case although a continuous reorganization occurs because of inward flow of filaments from the cell periphery (e.g., arrows in A and circled areas in C and E). (B, D, and F) Mobility diagrams depicting repetitive formation of fluorescent structures near the cell cortex (position of plasma membrane demarcated by black line) and subsequent inward movement in a cell of a confluent monolayer (B) or at free cell edges (D and F). Each diagram was obtained from a line extending from the outermost cell periphery (at right) to the outer KFs in the direction of the cell center (at left). The diagonal stripes show fluorescent structures (inverse presentation) that form in regular intervals at the cell edge and move inward in a continuous motion. Note the reduced frequency in B vs. D and F. Bars, 10 μm in A; 5 μm in B–F.

functional KF cytoskeletons and can be used to monitor the keratin system during the entire cell cycle under various experimental conditions (Windoffer and Leube, 1999, 2001; Strnad *et al.*, 2001, 2002, 2003). By time-lapse fluorescence imaging of one such cell line, i.e., vulva carcinoma-derived AK13-1 cells synthesizing chimera HK13-EGFP, we noted a continuous and inward-directed movement of keratin fluorescence originating from submembranous regions (Windoffer and Leube, 1999).

To find out whether this dynamic property of the KF system was a peculiar feature of A-431 cells or a more general phenomenon, we transfected several other epithelial cell types from different species with keratin-cDNAs. We observed in all instances the same type of centripetal movement of peripheral keratin fluorescence. The cells examined included human cell lines derived from hepatocellular carcinoma (PLC cells; Figures 1 and 2 and movies 1, 2, and 4), mammary adenocarcinoma (MCF7), and colon adenocarci-

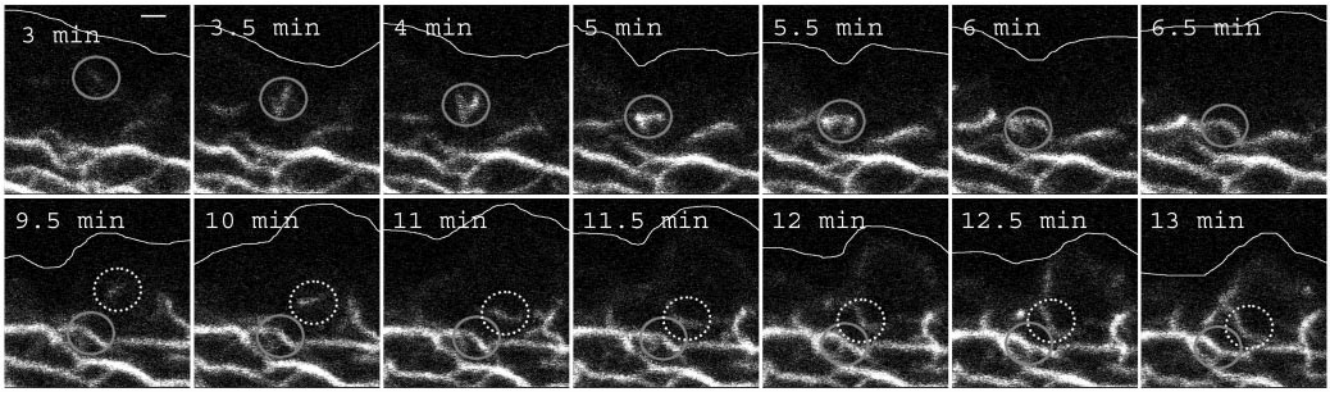

Figure 2. High-resolution confocal laser scanning microscopy depicting keratin dynamics in a peripheral region of a PK18–5 cell by detection of HK18-YFP fluorescence. Six focal planes are shown as superimposed projection views. A white line delineates the position of the plasma membrane; the nucleus is located below the depicted area. Note the formation of small granular material near the cell cortex, its enlargement into rods, the fusion with other fragments, and integration into the peripheral KF network. Circles highlight two examples of this process. The entire sequence is provided as movie 4. Bar, 1 μm.

noma (CaCo-2), immortalized human keratinocytes (HaCaT), human and murine primary keratinocytes (Figure 1; movie 3), and kidney-derived bovine MDBK and MDCK cells as well as rat kangaroo kidney PtK2 cells. To show that the documented phenomena were not specific features of particular keratins, cDNAs coding for fluorescent carboxyterminal fusions of human K5, K8, K13, K14, and K18 were expressed in some of these cell lines and the resulting dynamic behavior was compared. Notably, the same motility pattern was observed for all chimeras (compare, e.g., movies 1 and 2 with movie 3). To rule out that the position of the fluorescent protein tag affected the dynamic properties of the chimeric keratins, a cDNA coding for an aminoterminal fusion of human K14 was also examined (cf. Werner *et al.,* 2004). This chimera showed the same dynamic mobility as the carboxyterminal K14 fusion. Taken together, net inward movement of peripheral keratin appears to be a fundamental property of all epithelial cell types in culture.

To examine, whether inward-directed keratin mobility also occurs in nonepithelial cells, IF-free SW13 cells (Hedberg and Chen, 1986) were transfected with cDNA pairs coding for either HK8-CFP and HK18-YFP or HK5-CFP and HK14-YFP. In both cases, transfected cells formed extended KF networks. Live-cell imaging showed that, again, keratin fluorescence moves continuously from the most peripheral regions toward the cell center (Figure 3A; movie 5), suggesting that principles determining net inward flow of keratins are not restricted to epithelial cell types.

Keratin Particles Are Formed at Regular Intervals in the Cell Periphery and Move Centripetally toward the Peripheral Keratin Filament Network

A likely interpretation of the continuous inward flow of keratin fluorescence is that it reflects naturally occurring KF turnover. Hence, one would expect that KF precursors are generated in the cell periphery and are subsequently incorporated into the KF network. Therefore, we examined keratin dynamics within this region at high spatial and temporal resolution. Best results were obtained in the comparatively flat PLC cells. One example is illustrated in Figure 1C depicting the keratin distribution patterns in a membrane-proximal domain of stably cDNA-transfected cells synthesizing HK18-YFP. Here, as well as in other systems a ~2-μm region immediately adjacent to the plasma membrane was almost devoid of filamentous fluorescence except for desmosome-anchored filaments that traversed this space in tightly connected confluent cells. Starting approximately at 1-μm distance from the plasma membrane, weakly fluorescent and elongated structures were noted. These structures moved toward the existing KFs and became part of the KF network (circles in Figure 1C; movie 2). In most instances, the rodlet-like structures aligned with their longitudinal axis parallel to the plasma membrane.

To further analyze the peripheral keratin dynamics, mobility diagrams were prepared from the submembranous fluorescence (Figure 1, B, D, and F). Inward moving particles could thereby be recognized as oblique stripes originating in proximity to the plasma membrane and moving toward the cell center. In each instance, oblique traces were observed that were in parallel, indicating similar transport kinetics, and appeared at regular intervals to produce a characteristic Christmas tree-type pattern in which the trunk corresponds to the peripheral KFs and the branches to the inward-moving particles. This pattern was observed at various positions, suggesting that the entire cortex is capable of generating these structures. In confluent cells the frequency of particle formation (i.e., the distances between the branches) was ~20 min, whereas particle formation was more rapid at free cell edges (~5 min). In both instances, however, the movement was consistently unidirectional and without major stops. The average speed was between 100 and 300 nm/min and did not differ significantly between confluent cells and free cell borders (see also Windoffer and Leube, 1999).

In an attempt to elucidate further details of peripheral keratin particle dynamics, confocal laser scanning microscopy was performed. Representative sequences of altering fluorescence patterns are shown for a human primary keratinocyte producing fluorescent K14 (Figure 1E; movie 3) and a PK18–5 cell-synthesizing fluorescent K18 hybrids (Figure 2; movie 4). Best resolution was again achieved in PK18–5 cells in which very small granules of only a few pixels were first detected in close proximity to the plasma membrane (~1 μm). These granules elongated successively over a period of ~3.5 min while moving toward the cell center in a continuous motion before integration into the KF network.

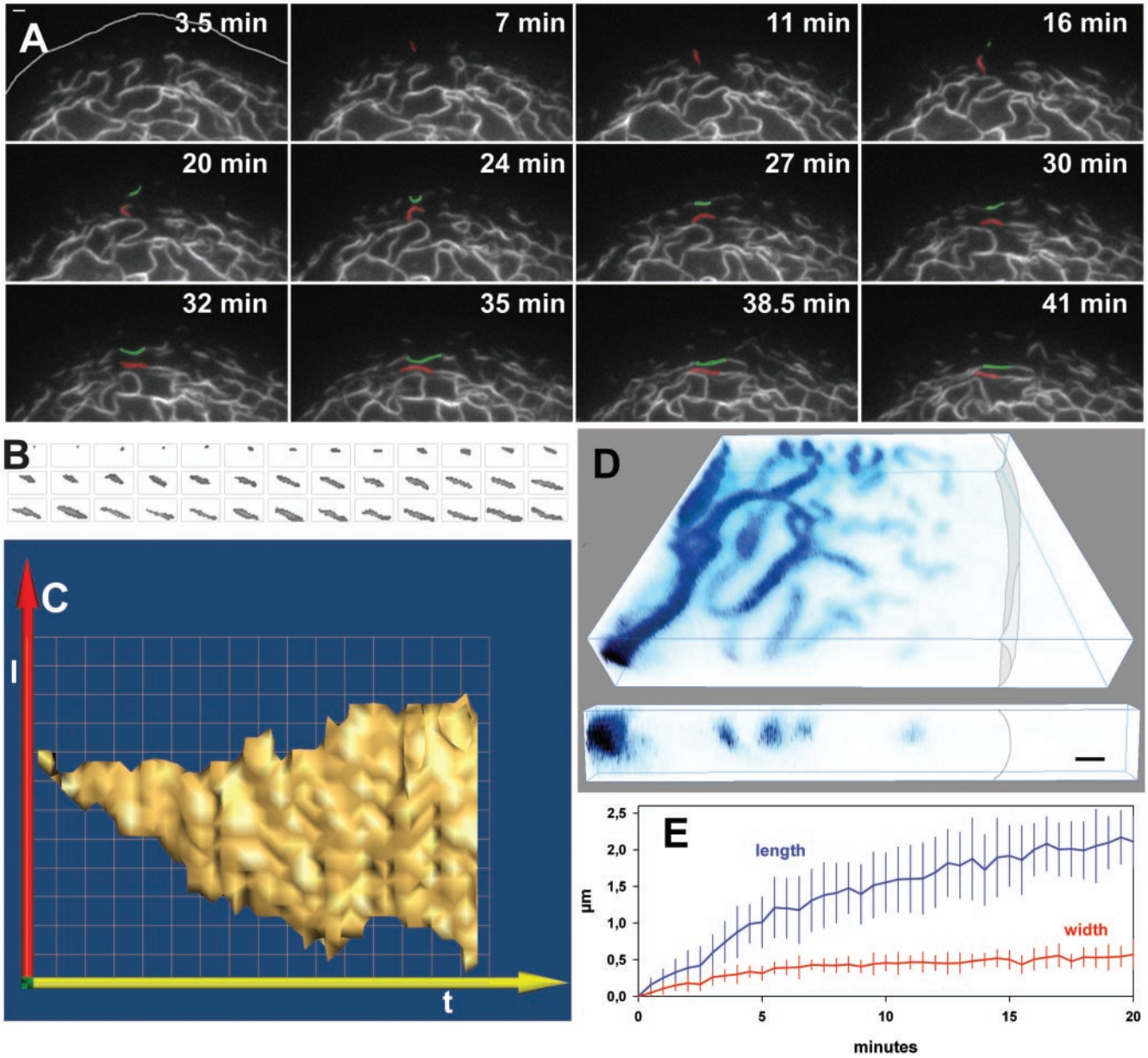

Figure 3. Details of KF network formation in living SW13 cells synthesizing HK8-CFP and HK18-YFP fluorescent hybrids. (A) Epifluorescence microscopy (detection of HK18-YFP) of a characteristic peripheral segment (position of plasma membrane indicated at 3.5 min) highlighting intermediate steps of KF network production. Two KF precursors are marked by color and followed until integration into the filament system. Note the formation of small granules below the cell surface that elongate, fuse, and become part of the KF network. The corresponding movie 5 shows further details. (B) Size changes of a single particle that was tracked from its first detection until integration into the network. For clarity's sake only the pixels associated with that particular particle are shown. Sampling frequency, 30 s. (C) The graph is derived from B, showing a surface view of the altering particle dimensions demonstrating a continuous, nonincremental particle elongation (l) before fusion with the KF network over time (t). (D) 3D reconstruction (voltex presentation) of the HK18-YFP fluorescence as recorded by confocal laser scanning microscopy of a peripheral region revealing spatial characteristics of various intermediates of filament assembly in relationship to intracellular topology (position of cell border demarcated). The volume of the top segment has the dimensions 20 × 20 × 3.5 μm. The bottom cube is a cross section to specifically highlight the increase in diameter of KF precursors only after integration into the peripheral KF network. (E) Plot summarizing the quantitative analysis of 10 time-space diagrams (see, e.g., C) depicting the increase in length (top graph) and diameter (bottom graph). Note the continuous elongation of particles during the entire 20 min in contrast to the increase in diameter that is limited to the first 5 min. Bars, SD. Bars, 1 μm in A and D.

Inward Moving Peripheral Keratin Particles Grow Continuously

To find out whether distinct intermediate steps could be defined that may either correspond to multiple unit length filaments (ULFs; Herrmann *et al.*, 2003) and/or squiggles (Helfand *et al.*, 2003), we examined the dimensions and growth characteristics of peripheral keratin structures in detail. Close inspection of the structures found in PLC cells (e.g., those labeled by circles in Figure 2) revealed continuous elongation of particles. The same process was observed

in IF-free SW13 cells after double transfection with cDNAs coding for fluorescent K8- and K18-hybrids (Figure 3A; movie 5). To characterize the genesis of particles more accurately, their alterations were examined at high resolution (e.g., Figure 3B). Time-space diagrams were prepared for each structure (n = 10; surface view of a typical diagram in Figure 3C). These diagrams showed that particles extended continuously in length, i.e., they elongated. The elongation kinetics were comparable for all particles with an overall growth rate of ~100 nm/min (Figure 3E). Furthermore, the growth rate was faster during the first 5 min (200 nm/min) than during the ensuing 15 min (<100 nm/min). After 15–25-min individual particles could not be tracked any more as they integrated into the filament network although inward motion of the peripheral network continued. Interestingly, particle diameter increased initially during the first 5 min, and remained stationary afterward until integration into the peripheral filament network (Figure 3E), where further increase in diameter was observed (cross section in Figure 3D). Taken together, it is concluded that particle growth is biphasic with an initial spherical extension of dot-like structures that is followed by elongation of filamentous rodlets until integration into the KF network.

Peripheral Keratin Particles Fuse with Each Other and Peripheral Keratin Filaments

The presumptive filamentous KF precursors were flexible structures, bending considerably although they were mostly aligned in parallel to the plasma membrane (Figures 2 and 3; movies 4 and 5). Close apposition of KF precursors led to fusion, and, in addition, KF precursors integrated directly into preexisting KFs after lateral apposition (e.g., top row in Figure 2 and Figure 3A). In all cases, the fusion involved only the ends of the KF precursors thereby leading to either end-to-end annealing of fragments or complete end-on integration of entire fragments into the KF network.

After integration of KF precursors, peripheral filaments enlarged into thicker filament bundles (e.g., Figure 3D) and continued to move centripetally. Filament bundles with the strongest fluorescence and the lowest mobility were either located in juxtanuclear domains or anchored at desmosomal cell-cell adhesion contact sites.

Keratin Filaments Are Predominantly Formed in the Cell Periphery

Our observations suggested that KFs are formed from nonfilamentous precursors in the cell periphery as small particles that elongate and fuse while moving toward the cell center. To verify these assumptions and to assess the importance of this process for KF turnover, FRAP experiments were performed. A representative experiment is shown in Figure 4 and movie 6. In this instance, a segment of the peripheral cytoplasm was bleached and the recurrence of fluorescence was monitored at regular intervals. Peripheral filaments reformed after 1 h, whereas the more centrally located filaments were still mostly devoid of fluorescence at this time. Graphic representation of reappearing fluorescence in relation to time and intracellular topology is shown in the bottom panel of Figure 4, highlighting that the peripheral fluorescence concentrated first in filaments in the outer cytoplasm (highest peak), although some low-level fluorescence recovery occurred throughout the entire network. Taking into account that, at steady state, fluorescence intensity is stronger in the more central parts of the cytoplasm with its thick filament bundles, these results are quite significant. It is therefore concluded that the lateral exchange of subunits throughout the entire length of the KF system is quantitatively only the minor way of network renewal in these cells, whereas peripheral replenishment is the major mode of KF turnover. Similar results were obtained in other cell types (unpublished data). Furthermore, the bleaching experiments provided positive evidence that the peripheral keratin fragments are generated from soluble keratins and that they are the building blocks of newly forming filaments.

In an attempt to track the entire life cycle of KFs, including not only the formation of KF bundles but also their disassembly, we bleached cells completely except for small peripheral segments containing the presumptive KF precursors and newborn KFs (Figure 5). For quantification two areas of interest were defined: area 1 encompassing the residual fluorescence in the cell periphery together with the adjacent centripetal region and area 2 corresponding to a completely bleached part of the cytoplasm. As predicted, peripheral concentration of fluorescent material into filament bundles that moved toward the nucleus was detectable in area 1. Remarkably, the absolute amount of fluorescence within this region remained almost the same for 70 min, indicating lack of significant release of subunits into the soluble pool and/or exchange of keratin polypeptides with other distant filament bundles. Subsequently, gradual fluorescence fading of KF bundles and a decline of the overall fluorescence occurred within area 1 (Figure 5, B and C). This decline was in contrast to the slow increase in fluorescence in the completely bleached area 2, suggesting a net flow of fluorescent material from the fluorescent KF bundles to the rest of the cytoplasm. Furthermore, the fluorescence increase in area 2 showed similar kinetics as the fluorescence recovery in completely bleached control cells (Figure 5C) where it reflects the rate of keratin biosynthesis. Based on quantification of fluorescence recovery in these completely bleached cells, the rate of synthesis was estimated to be ~2%/h, which is in accordance with previous reports of comparatively long half-lives of keratins (Denk *et al.*, 1987; Kulesh and Oshima, 1988). This low de novo synthetis is clearly not sufficient to account for the continuously ongoing KF formation in the cell periphery, indicating that subunits must circulate between existing filaments and the soluble pool to sustain this process. Taken together, our observations show that the KF network possesses different subdomains: a peripheral region consisting of young filaments that are continuously replenished by integration of KF precursors, which are recruited from the soluble pool, and a region closer to the nucleus with older filaments, some of which are disassembled to support peripheral network renewal. This "aging" process is coupled to continuous inward movement.

Renewal of the Keratin Filament System after Complete Destruction Originates from the Cell Periphery

A prediction of the results obtained in the FRAP experiments was that de novo KF network formation may also arise from the cell periphery. Consistent with this idea, we have previously shown that reformation of the KF system after mitosis originates from the cell cortex in AK13–1 cells (Windoffer and Leube, 2001). To test whether de novo KF network formation is also dictated by the cell periphery during interphase, the KF system was disassembled in AK13-1 cells by transient treatment with the tyrosine phosphatase inhibitor orthovanadate. After short drug treatment, network reformation occurred within <1 h (Strnad *et al.*, 2002), whereas other treatment protocols (e.g., longer incubation periods, higher drug concentration) prevented reformation either partially (Figure 6A) or almost completely (Figure 6B). In cells with partial recovery after a short pulse of orthovanadate, granular and filamentous structures were

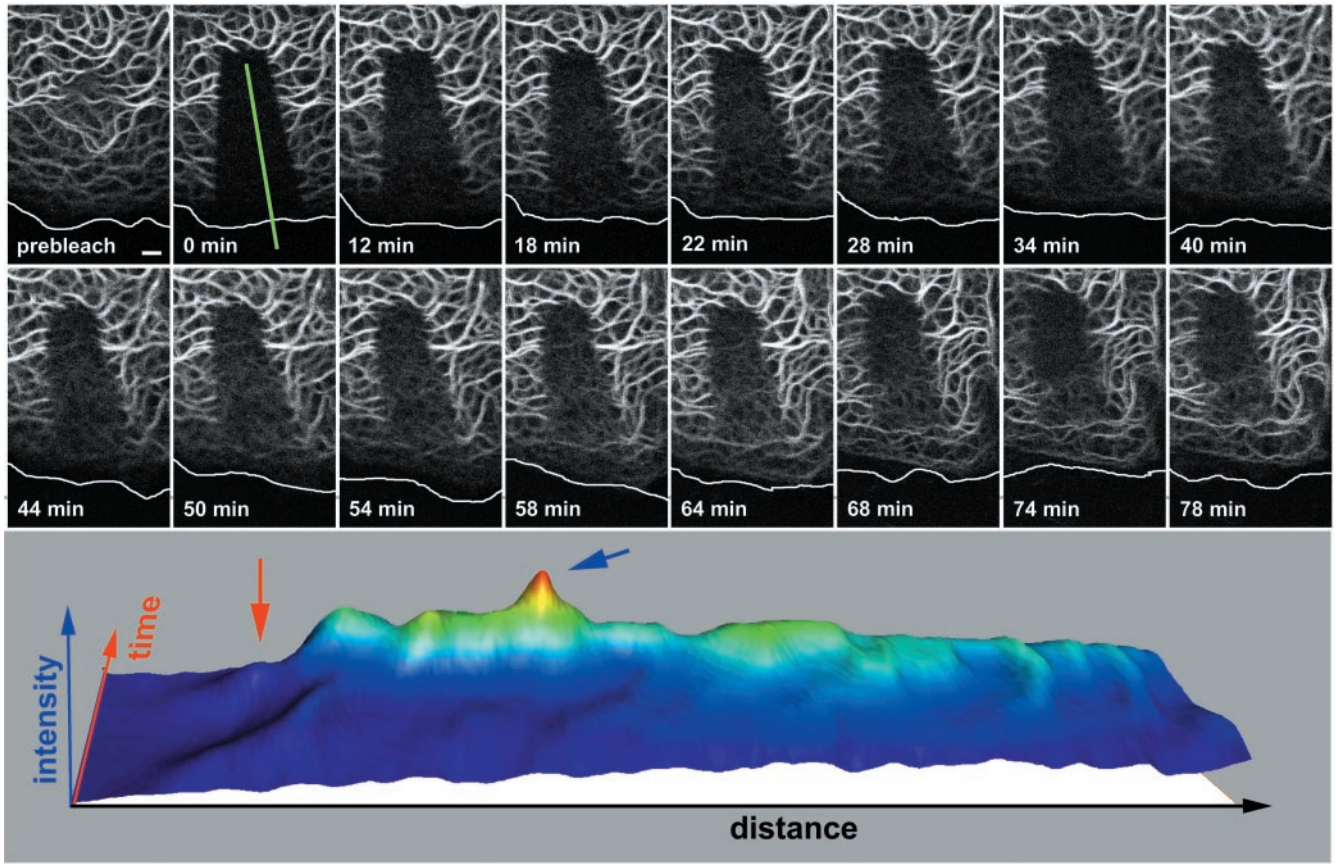

Figure 4. FRAP analysis of a PK18–5 cell elucidating the differential recovery of central and peripheral KFs. The first picture shows a confocal fluorescence image of a peripheral region depicting the strongly fluorescent and more central KFs at top and the more weakly fluorescent peripheral KFs at bottom (position of plasma membrane demarcated by white line). The postbleach fluorescence image is shown at time point 0 min and the recovery of fluorescence is documented at different intervals (complete series provided as movie 6). Note the recurrence of fluorescence predominantly in the cortical region where distinct inward moving filaments can be distinguished. Bar, 2 μm. The 3D diagram in the bottom panel shows alterations of fluorescence intensity that was measured along a line (*distance*; for position of line see 0 min on top) over time. Note that the vast majority of fluorescence recurs in the periphery originating beneath the plasma membrane (red arrow) and reaching peak values (blue arrow) at positions where filaments are first distinguishable.

first seen in the cell periphery where they were detected as mobile entities continuously moving inward but disappearing at the innermost edge of a circumscribed peripheral domain without forming a sustainable network (Figure 6A; movie 7). This suggests that additional factors needed for network formation were still inactivated or not present. Interestingly, the keratin granules and KFs were confined to the same peripheral region where KF precursors are usually found (compare Figure 6A with Figures 1–5).

In another instance, when granules were predominantly formed in the cell periphery in the continued presence of orthovanadate, high-resolution time-lapse epifluorescence microscopy revealed further details (Figure 6B; movie 8). Small granular particles were seen to originate from the outermost part of the cytoplasm <2 μm away from the plasma membrane. These granules elongated into filaments and/or grew into larger granules that were frequently connected by thin filamentous threads. The interconnected particles moved further toward the cell center up to an imaginary line where the large, spheroidal granules disappeared rapidly within <5 min (Figure 6, B and C). In most instances, granules lost their interior first, forming hollow spheres with sidewise extending filaments, and were only then disassembled completely (arrowheads in Figure 6B).

Peripheral Keratin Filament Re-formation Does Not Depend on Desmosomes

Finally, we examined the contribution of desmosomes to KF network reformation in cells that typically contain extensive desmosomal contact sites. For this purpose we used the previously described A-431 subline B5, which stably produces a dominant-negative desmoglein mutant (Troyanovsky *et al.*, 1993). These cells not only lack desmosomes but are also characterized by a collapsed KF system that is concentrated in perinuclear whorl-like structures, indicating loss of the characteristic transcellular network continuity. When fluorescent keratin chimeras were expressed in these cells, the characteristic centripetal inward-directed mobility of keratin precursors was again detected in the broadened peripheral zone (Figure 7; movie 9), showing that desmosomes are not needed for peripheral KF network renewal.

DISCUSSION

Detection of a Novel Mechanism of Keratin Filament Network Turnover

We conclude from the following observations that turnover and de novo formation of the KF network originate predom-

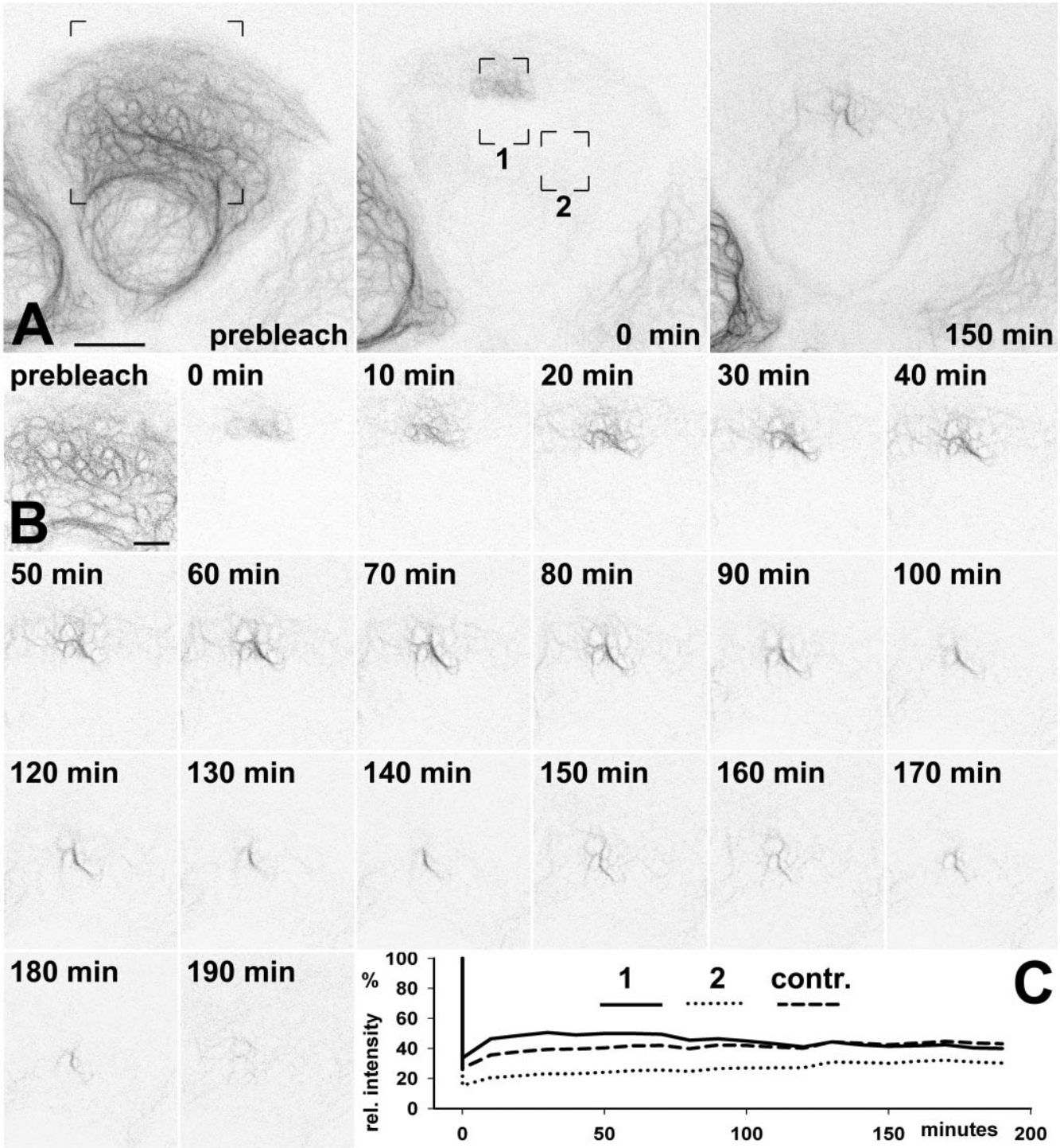

Figure 5. FRAP-analysis of a PK18–5 cell depicting formation and disappearance of KF bundles. (A and B) The series of inverse fluorescence micrographs show either the projection of all 11 recorded planes (A) or only a single plane (B). Images were recorded by confocal laser scanning microscopy at 10-min intervals using a large pinhole and low laser power. (A) Survey views showing the fluorescence distribution before bleaching (prebleach), immediately afterward (0 min), and after 2.5-h recovery (150 min). Almost the entire cell was bleached leaving only a small peripheral region unbleached. Note, that filamentous material is concentrated in a juxtanuclear position after 2.5 h. (B) High-power view of the area demarcated in A revealing details of filament bundle formation. Immediately after bleaching only very fine fluorescence is visible, which subsequently concentrates into strongly fluorescent filamentous structures within the next 90 min. At the end of the recording, the filament bundles have moved toward the nucleus and lost most of their fluorescence. Bars, 10 μm in A; 2 μm in B. (C) Graph showing the total fluorescence intensity measured as percentage of the prebleach intensity in all focal planes of the regions delineated in A and in a cell that was completely bleached (*contr.*). Note the slow and comparable increase in fluorescence in region 2 and the control in contrast to the slow decrease of fluorescence in region 1.

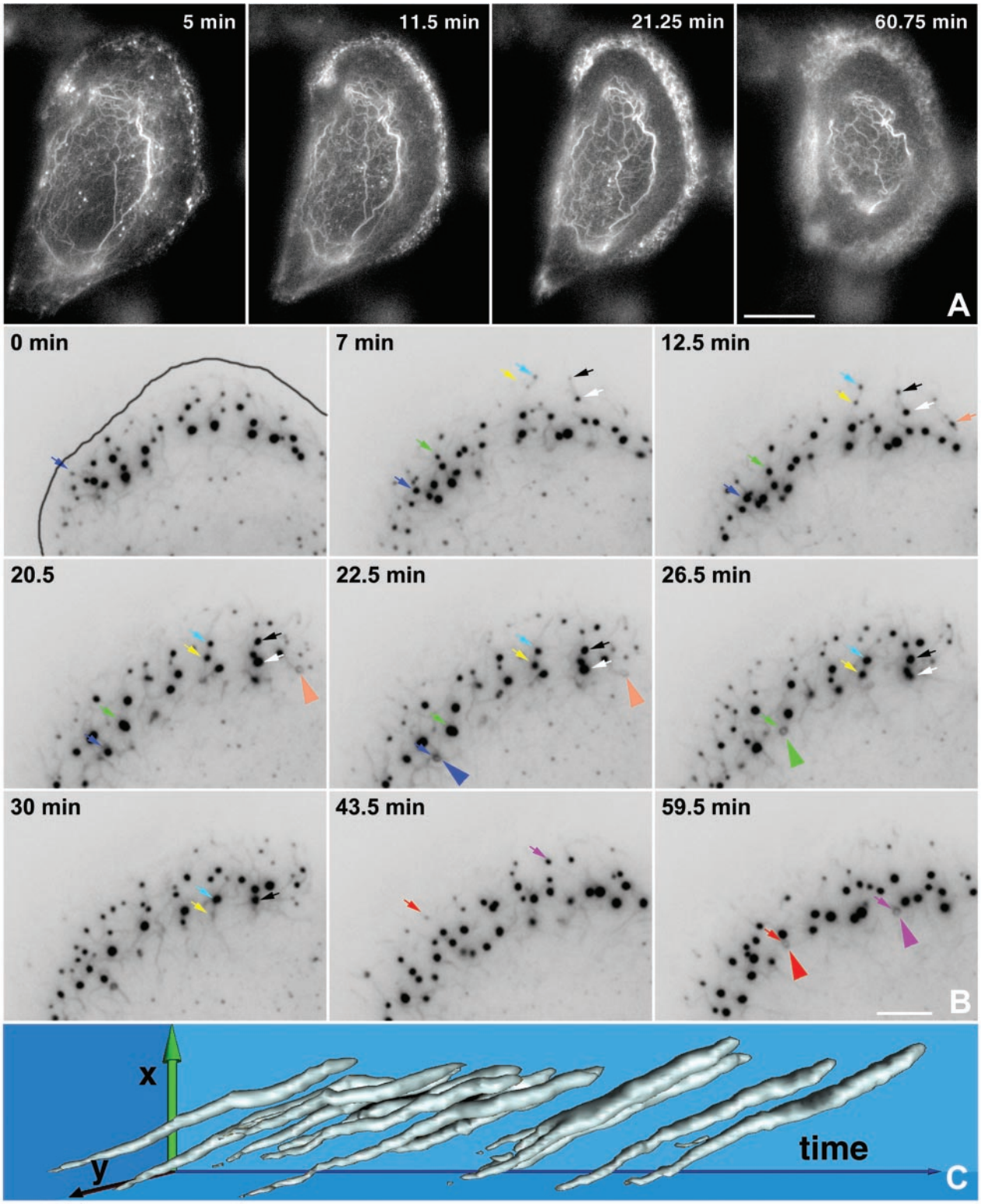

Figure 6. Fluorescence micrographs showing details of keratin dynamics in the cell periphery of AK13–1 cells synthesizing HK13-EGFP after orthovanadate treatment. (A) Cells were incubated with orthovanadate (10 mM) for 4 min before imaging resulting in disassembly of most of the KF network and leaving only some perinuclear bundles. Images were recorded every 30 s and are provided as movie 7. Note the high turnover of material in the cell periphery where granules are formed at early time points and fine filamentous material is generated later. All material exhibits continuous inward motion and is disassembled at the central margin of a distinct peripheral domain. (B) Peripheral region showing HK13-EGFP fluorescence (inverse presentation) of another AK13–1 cell treated with 10 mM orthovanadate. Small granules are formed underneath the plasma membrane and are connected by thin filament bridges. Granules further grow and move toward the cell center (see color-coded arrows) but disappear by disassembly from the granule interior (color-coded arrowheads). For details see also movie 8. Bars, 10 μm in A; 5 μm in B. (C) Time-space diagram of a region selected from B showing the time course of granule formation with continuous enlargement and sudden disassembly at a sharp transition zone.

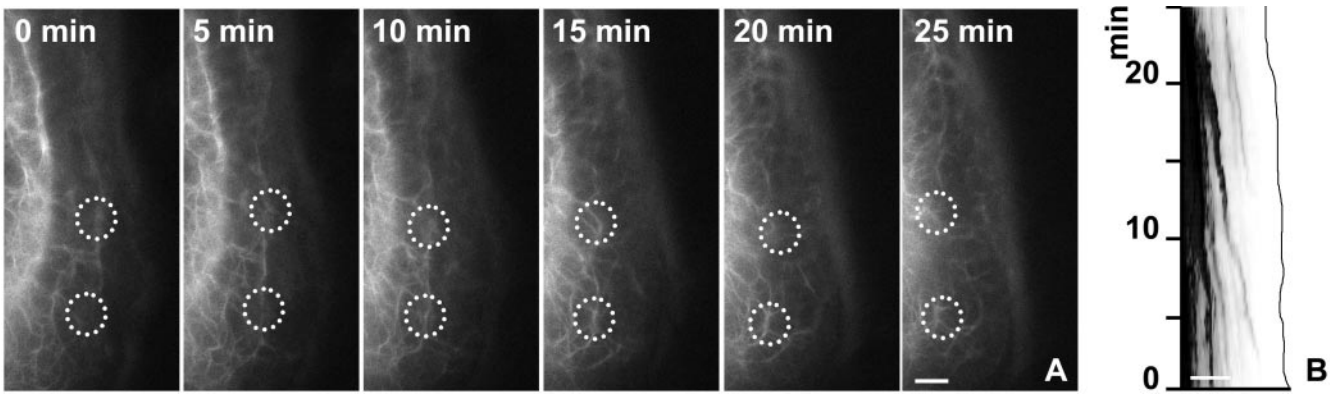

Figure 7. Keratin dynamics in desmosome-free A-431 cells (clonal subline B5 stably transfected with CoDg-cDNA) that was, in addition, transiently cDNA transfected to synthesize HK13-EGFP. Plasma membrane to the right (black line in B), nucleus to the left. Peripheral filamentous structures are encircled to highlight inward directed movement in A as also evident from the mobility diagram in B (inverse presentation). Complete sequence is shown as movie 9. Bars, 5 μm.

inantly in a specialized compartment in the cell periphery: i) Keratin particles are continuously generated in proximity to the plasma membrane and move toward the existing KF network into which they integrate (Figures 1–3). ii) Recurrence of distinct filamentous fluorescence after photobleaching of cell segments is first seen in the cell periphery (Figure 4). iii) FRAP experiments, in which cells are completely bleached with the exception of a small subcortical segment, show that KF bundles are generated peripherally and translocate toward the cell center (Figure 5). iv) Partial KF network reformation after complete disruption by the tyrosine phosphatase inhibitor orthovanadate is detected in a distinct zone beneath the plasma membrane (Figure 6). v) De novo KF network formation occurs after complete breakdown during mitosis and originates exclusively from the cell cortex (Windoffer and Leube, 2001). vi) *Epidermolysis bullosa simplex*–type mutant keratins with disturbed KF formation form short-lived granules that are restricted to peripheral cellular domains (Werner *et al.,* 2004).

Our conclusions are in contrast to the view that KF turnover occurs primarily by lateral exchange of subunits throughout the entire length without topological preference in epithelial cells (Miller *et al.,* 1991, 1993; Yoon *et al.,* 2001; Helfand *et al.,* 2003) and in nonepithelial cells ectopically producing KFs (Kreis *et al.,* 1983; Bader *et al.,* 1991), which is also supported by observations on the vimentin system (Vikstrom *et al.,* 1989, 1992; Ngai *et al.,* 1990; Sarria *et al.,* 1990; Coleman and Lazarides, 1992). In contrast to most of those previous investigations, our results are based on direct monitoring of keratin dynamics in stably transfected epithelial cells that are at equilibrium and contain by all accounts a normal keratin cytoskeleton. The fluorescent keratins amount to <20% of total keratins as estimated from gel-electrophoretically separated and Coomassie-blue–stained cytoskeletal preparations and are integrated into a functionally and structurally competent KF network (Windoffer and Leube, 1999; Strnad *et al.,* 2002). Furthermore, different concentrations of fluorescent keratin chimeras (always <20% of total insoluble keratin) in a number of stably transfected cell lines (this study; Windoffer and Leube, 1999, 2001; Strnad *et al.,* 2001, 2002) do not affect keratin behavior. In addition, the low biosynthetic rate of the chimeras is in agreement with the long half-lives of wild-type keratins (Denk *et al.,* 1987; Kulesh and Oshima, 1988).

Taking also into account that N- and C-terminally tagged hybrids exhibit similar behavior and that the fluorescent chimeras codistribute topologically and biochemically exactly with the endogenous keratins (Windoffer and Leube, 1999), we are quite confident that the reported keratin turnover dynamics reflect the situation of endogenous keratins, although the kinetics in cultured cell systems might differ from tissues and living organisms. In contrast, the lateral exchange model of KF network renewal is primarily based on experiments in which large amounts of keratins were introduced, e.g., by microinjection of labeled polypeptides or transient transfection (Miller *et al.,* 1991, 1993; Yoon *et al.,* 2001). Thus, the very large amounts of foreign keratin polypeptides may have uncovered alternative routes of KF turnover that are less prominent during steady state. A similar out-of-balance situation was also encountered in orthovanadate-treated cells in which cytoskeleton-anchored granules formed filaments throughout the cytoplasm (Strnad *et al.,* 2002). Therefore, the equilibrium between both types of keratin turnover may be subject to regulation.

Initiation of Keratin Filament Precursor Formation

The first particulate keratin fluorescence is detectable in peripheral cytoplasmic domains that are <1 μm away from the plasma membrane (step 1 in Figure 8). The size of these initial keratin particles is difficult to estimate given the resolution limit of our images with a pixel size of 100 × 100 nm. It will therefore require improved technology to decide whether the 60-nm-long ULFs exist in vivo (Herrmann *et al.,* 1999, 2002, 2003; Strelkov *et al.,* 2003) and whether they are joined together to form longitudinal poly-ULFs as suggested recently (Herrmann *et al.,* 2003).

Our observations of selective KF formation in the cell periphery indicate that cortical factors exist that determine the initiation of KF precursor formation. It is unlikely that desmosomal components are involved, because peripheral KF network formation occurs in keratin cDNA-transfected nonepithelial cells such as IF-free SW13 cells, and KF turnover continues in cells with disrupted desmosomes, although a participation of internalized and/or immature cytoplasmic desmosomal particles cannot be formally excluded. Potential "initiation" factors include plectin, which is enriched in the cortex of certain cells (Eger *et al.,* 1997; Strnad *et al.,* 2002), and localizes to keratin granules with filament-formation capacity (Strnad *et al.,* 2002), membrane-associated and keratin-binding proteins such as KAP85 (Chou *et al.,* 1994) and lipocortin 1/annexin 1 (Croxtall *et al.,* 1998), and enzymatic activities that are restricted to

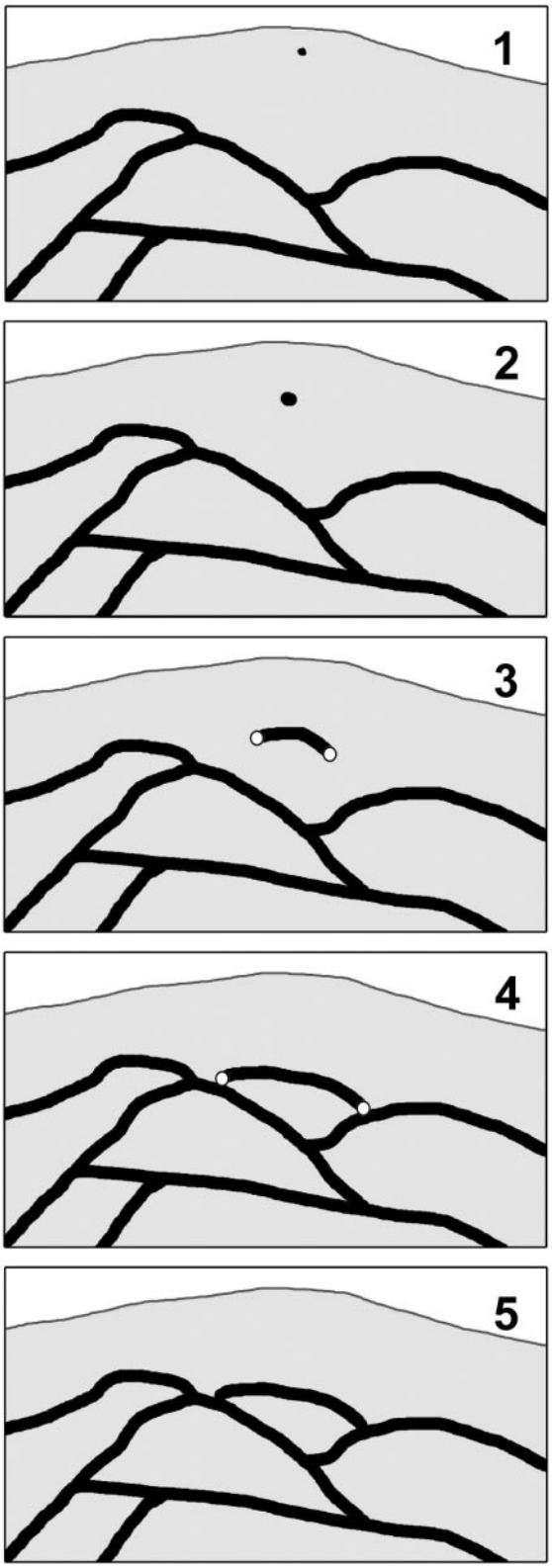

Figure 8. Scheme summarizing initial steps of KF formation in the peripheral cytoplasm. Small particles are first detected in proximity to the plasma membrane (1) which enlarge into spheroidal granules (2) and elongate into rodlets (3). The fusion-competent ends of rodlets associate with peripheral filaments (4) and integrate into the KF network (5). For further details see DISCUSSION.

a membrane-proximal region and regulate the degree of keratin phosphorylation (review in Omary *et al.,* 1998). Furthermore, dynamic polymerization platforms may exist that also include F-actin as proposed by Weber and Bement (2002). Given the strong tendency of keratins to rapidly form KFs in vitro (Herrmann *et al.,* 1999, 2002), absence of factors that prevent KF assembly in the cortex may be an alternative mechanism by which KF formation is confined to the cell periphery. Of note, 14-3-3 proteins have been suggested to act as keratin solubilizers by associating with soluble, hyperphosphorylated KF subunits (Liao and Omary, 1996) and thereby affecting keratin organization (Ku *et al.,* 2002).

Growth of Keratin Filament Precursors

We were able, for the first time, to directly monitor the growth of KF precursors in living cells during interphase. Growth of keratin particles was biphasic and occurred simultaneously with their transport toward the cell interior. The initial growth phase of dot-like particles was characterized by spherical particle enlargement (step 2 in Figure 8), which may be initiated by cortical initiation factor(s). The second growth phase resulted in elongation of filamentous/rod-like particles (step 3 in Figure 8), presumably by longitudinal annealing of KF subunits. The transition between both growth phases appears to be subject to regulation, because formation of peripheral filamentous KF precursors is inhibited during mitosis (Windoffer and Leube, 1999, 2001) and is disturbed in cells that are either treated with certain phosphatase inhibitors (Strnad *et al.,* 2001) or produce *Epidermolysis bullosa simplex*–type keratin mutations (Coulombe *et al.,* 1991a, 1991b; Werner *et al.,* 2004). In these instances, large spheroidal granules are formed and elongated filamentous KF precursors are not generated (Strnad *et al.,* 2001; Werner *et al.,* 2004). Yet, granule formation is not irreversible and elongation of granular material has been documented in several instances for keratins in epithelial cells (Miller *et al.,* 1991, 1993; Strnad *et al.,* 2001, 2002; Windoffer and Leube, 2001; Werner *et al.,* 2004) and nonepithelial cells (Kreis *et al.,* 1983; Franke *et al.,* 1984) and also for vimentin under certain conditions (Vikstrom *et al.,* 1989; Bridger *et al.,* 1998; Prahlad *et al.,* 1998; Reichenzeller *et al.,* 2000). Interestingly, keratin granules and filamentous KF precursors can coexist as observed not only in orthovanadate-treated cells (this study), cells expressing mutant keratins (e.g., Coulombe *et al.,* 1991a, 1991b; Werner *et al.,* 2004), or injured hepatocytes (cf. Cadrin and Martinoli, 1995) but also in normal cells (Liovic *et al.,* 2003), providing support for the idea that certain rate-limiting factors determine the choice between both keratin polymer configurations.

The KF precursors described here most likely correspond to the squiggles characterized by others (Yoon *et al.,* 2001; Helfand *et al.,* 2003). KF precursors/squiggles differ, however, from vimentin and axonal neurofilament squiggles (Prahlad *et al.,* 1998; Roy *et al.,* 2000; Wang *et al.,* 2000; Wang and Brown, 2001; Helfand *et al.,* 2003) in their motility: they do not exhibit saltatory mobility (this study), they move exclusively toward the cell center without significant bidirectional movement (this study; Yoon *et al.,* 2001), and they are much slower at 100–300 nm/min (this study; Windoffer and Leube, 1999; Yoon *et al.,* 2001) in comparison to the 1–2 μm/s measured for vimentin and neurofilament squiggles (Prahlad *et al.,* 1998; Roy *et al.,* 2000; Wang *et al.,* 2000; Wang and Brown, 2001). Instead, KF precursors exhibit continuous inward motion in all instances, which is reminiscent of the treadmilling of the actin system (Theriot, 1997; Carlier, 1998; Small *et al.,* 2002; Vaezi *et al.,* 2002).

Integration of Keratin Filament Precursors into the Keratin Filament Network

Important functional features of the continuously growing keratin precursors are their fusion-competent ends, which are not only able to recruit further IF subunits (elongation), but also fuse with ends of other keratin precursors to generate much larger fragments, and, most importantly, integrate end-on into the existing IF cytoskeleton without disruption of its continuity (steps 4 and 5 in Figure 8). In the absence of central filaments and in instances when filament polymers are unable to integrate into the filament system fusion events occur and the material is either subject to rapid turnover (Figure 6; Windoffer and Leube, 2001; Strnad *et al.*, 2002; Werner *et al.*, 2004) or gives rise to de novo KF network formation from the cell periphery in certain instances (Windoffer and Leube, 1999, 2001; Strnad *et al.*, 2002).

The restriction of KF precursors to a circumscribed region of the cell periphery identifies a novel domain that is functionally and structurally organized in a vectorial manner extending from the plasma membrane where KF precursor formation is initiated to a morphologically ill-defined zone several micrometers away where elongated KF precursors integrate into preexisting KFs. This novel compartment corresponds, at least in part, to the zone that is delineated in cells treated with the tyrosine phosphatase inhibitor orthovanadate (Figure 6) in which keratin granules are formed.

Similarly, keratin granules containing *Epidermolysis bullosa simplex*–type keratin mutants in cDNA-transfected epithelial cells and keratinocytes derived from transgenic mice are also restricted to this region (Coulombe *et al.*, 1991a, 1991b; Werner *et al.*, 2004). Remarkably, granules are rapidly disassembled at the inner border of the peripheral compartment in a distinct zone (Figure 6; Werner *et al.*, 2004) whose position may vary considerably as shown for A-431 cells lacking desmosomes. We do not know the molecular determinants of this novel functional cellular domain but consider it possible that it is delineated by inward-directed actin fibers that are in motion by treadmilling (Carlier, 1998; Small *et al.*, 2002; Vaezi *et al.*, 2002).

CONCLUSIONS

Taken together, we conclude that the submembranous region of epithelial cells fulfils crucial organizing functions for the KF system. An important consequence of the detected peripheral mode of KF network turnover is that the intrinsically nonpolar KF system acquires spatial orientation, i.e., a peripheral → central organization in which young filaments are in the cell periphery and old filaments are in the perinuclear domain. The more dynamic peripheral filaments may thus be capable to react to particular structural and functional requirements imposed on the cytoskeleton, whereas the more stable central filaments—probably together with the rather stable desmosome-anchored filaments—may be primarily responsible for the continuous mechanical stability of epithelial tissues. This arrangement is advantageous, because peripheral parts of the cell are the primary targets of cell shape changes. Because all epithelial tissues are subject to continuous remodelling as a result of proliferation, cell death or adaptation to mechanical requirements, maintenance of tissue integrity and homeostasis is a constant challenge that relies on continuous cross talk between the environment and the cytoskeleton. We think that the plasma membrane and the adjacent cytoplasmic region are ideally suited to mediate this cross-talk by receiving signals from outside and transforming them into alterations of KF turnover and organization. The future challenge is to find out whether similar organizational principles apply also to other IF systems as may be concluded from the detection of vimentin squiggles in peripheral regions lacking mature IFs (Ho *et al.*, 1998; Prahlad *et al.*, 1998; Yoon *et al.*, 1998; Martys *et al.*, 1999) and the presence of a highly dynamic pool of neurofilament subunits in growth cones that has been proposed to participate in filament formation (Chan *et al.*, 2003).

ACKNOWLEDGMENTS

We thank Drs. Harald Herrmann (German Cancer Research Center, Heidelberg, Germany) and Nicola Werner (Bonn University, Germany) for generous gifts of DNA constructs, and Dr. Gerd Technau (Mainz University) for use of the confocal microscope. The expert technical support Ursula Wilhelm is also gratefully acknowledged. This work was supported by the "Stiftung Rheinland-Pfalz für Innovation" during initial phases and by the German Research Council (LE 566/7).

REFERENCES

Albers, K., and Fuchs, E. (1987). The expression of mutant epidermal keratin cDNAs transfected in simple epithelial and squamous cell carcinoma lines. J. Cell Biol. *105,* 791–806.

Bader, B.L., Magin, T.M., Freudenmann, M., Stumpp, S., and Franke, W.W. (1991). Intermediate filaments formed de novo from tail-less cytokeratins in the cytoplasm and in the nucleus. J. Cell Biol. *115,* 1293–1307.

Bologna, M., Allen, R., and Dulbecco, R. (1986). Organization of cytokeratin bundles by desmosomes in rat mammary cells. J. Cell Biol. *102,* 560–567.

Boukamp, P., Petrussevska, R.T., Breitkreutz, D., Hornung, J., Markham, A., and Fusenig, N.E. (1988). Normal keratinization in a spontaneously immortalized aneuploid human keratinocyte cell line. J. Cell Biol. *106,* 761–771.

Bridger, J.M., Herrmann, H., Munkel, C., and Lichter, P. (1998). Identification of an interchromosomal compartment by polymerization of nuclear-targeted vimentin. J. Cell Sci. *111,* 1241–1253.

Cadrin, M., and Martinoli, M.G. (1995). Alterations of intermediate filaments in various histopathological conditions. Biochem. Cell Biol. *73,* 627–634.

Carlier, M.F. (1998). Control of actin dynamics. Curr. Opin. Cell Biol. *10,* 45–51.

Celis, J.E., Small, J.V., Larsen, P.M., Fey, S.J., De Mey, J., and Celis, A. (1984). Intermediate filaments in monkey kidney TC7 cells: focal centers and interrelationship with other cytoskeletal systems. Proc. Natl. Acad. Sci. USA *81,* 1117–1121.

Chan, W.K., Yabe, J.T., Pimenta, A.F., Ortiz, D., and Shea, T.B. (2003). Growth cones contain a dynamic population of neurofilament subunits. Cell Motil. Cytoskel. *54,* 195–207.

Chou, C.F., Riopel, C.L., and Omary, M.B. (1994). Identification of a keratin-associated protein that localizes to a membrane compartment. Biochem. J. *298,* 457–463.

Coleman, T.R., and Lazarides, E. (1992). Continuous growth of vimentin filaments in mouse fibroblasts. J. Cell Sci. *103,* 689–698.

Coulombe, P.A., Hutton, M.E., Letai, A., Hebert, A., Paller, A.S., and Fuchs, E. (1991a). Point mutations in human keratin 14 genes of epidermolysis bullosa simplex patients: genetic and functional analyses. Cell *66,* 1301–1311.

Coulombe, P.A., Hutton, M.E., Vassar, R., and Fuchs, E. (1991b). A function for keratins and a common thread among different types of epidermolysis bullosa simplex diseases. J. Cell Biol. *115,* 1661–1674.

Coulombe, P.A., and Omary, M.B. (2002). 'Hard' and 'soft' principles defining the structure, function and regulation of keratin intermediate filaments. Curr. Opin. Cell Biol. *14,* 110–122.

Croxtall, J.D., Wu, H.L., Yang, H.Y., Smith, B., Sutton, C., Chang, B.I., Shi, G.Y., and Flower, R. (1998). Lipocortin 1 co-associates with cytokeratins 8 and 18 in A549 cells via the N-terminal domain. Biochim. Biophys. Acta *1401,* 39–51.

Denk, H., Lackinger, E., Zatloukal, K., and Franke, W.W. (1987). Turnover of cytokeratin polypeptides in mouse hepatocytes. Exp. Cell Res. *173,* 137–143.

Eckert, B.S., Daley, R.A., and Parysek, L.M. (1982). Assembly of keratin onto PtK1 cytoskeletons: evidence for an intermediate filament organizing center. J. Cell Biol. *92,* 575–578.

Eger, A., Stockinger, A., Wiche, G., and Foisner, R. (1997). Polarisation-dependent association of plectin with desmoplakin and the lateral submembrane skeleton in MDCK cells. J. Cell Sci. *110,* 1307–1316.

Franke, W.W., Schmid, E., Mittnacht, S., Grund, C., and Jorcano, J.L. (1984). Integration of different keratins into the same filament system after microinjection of mRNA for epidermal keratins into kidney epithelial cells. Cell *36,* 813–825.

Georgatos, S.D., and Blobel, G. (1987). Two distinct attachment sites for vimentin along the plasma membrane and the nuclear envelope in avian erythrocytes: a basis for a vectorial assembly of intermediate filaments. J. Cell Biol. *105,* 105–115.

Georgatos, S.D., Weber, K., Geisler, N., and Blobel, G. (1987). Binding of two desmin derivatives to the plasma membrane and the nuclear envelope of avian erythrocytes: evidence for a conserved site-specificity in intermediate filament-membrane interactions. Proc. Natl. Acad. Sci. USA *84,* 6780–6784.

Hager, B., Bickenbach, J.R., and Fleckman, P. (1999). Long-term culture of murine epidermal keratinocytes. J. Invest. Dermatol. *112,* 971–976.

Hedberg, K.K., and Chen, L.B. (1986). Absence of intermediate filaments in a human adrenal cortex carcinoma-derived cell line. Exp. Cell Res. *163,* 509–517.

Helfand, B.T., Loomis, P., Yoon, M., and Goldman, R.D. (2003). Rapid transport of neural intermediate filament protein. J. Cell Sci. *116,* 2345–2359.

Herrmann, H., Haner, M., Brettel, M., Ku, N.O., and Aebi, U. (1999). Characterization of distinct early assembly units of different intermediate filament proteins. J. Mol. Biol. *286,* 1403–1420.

Herrmann, H., Hesse, M., Reichenzeller, M., Aebi, U., and Magin, T.M. (2003). Functional complexity of intermediate filament cytoskeletons: from structure to assembly to gene ablation. Int. Rev. Cytol. *223,* 83–175.

Herrmann, H., Wedig, T., Porter, R.M., Lane, E.B., and Aebi, U. (2002). Characterization of early assembly intermediates of recombinant human keratins. J. Struct. Biol. *137,* 82–96.

Ho, C.L., Martys, J.L., Mikhailov, A., Gundersen, G.G., and Liem, R.K. (1998). Novel features of intermediate filament dynamics revealed by green fluorescent protein chimeras. J. Cell Sci. *111,* 1767–1778.

Hofmann, I., and Franke, W.W. (1997). Heterotypic interactions and filament assembly of type I and type II cytokeratins in vitro: viscometry and determinations of relative affinities. Eur. J. Cell Biol. *72,* 122–132.

Knapp, L.W., O'Guin, W.M., and Sawyer, R.H. (1983). Drug-induced alterations of cytokeratin organization in cultured epithelial cells. Science *219,* 501–503.

Kreis, T.E., Geiger, B., Schmid, E., Jorcano, J.L., and Franke, W.W. (1983). De novo synthesis and specific assembly of keratin filaments in nonepithelial cells after microinjection of mRNA for epidermal keratin. Cell *32,* 1125–1137.

Ku, N.O., Michie, S., Resurreccion, E.Z., Broome, R.L., and Omary, M.B. (2002). Keratin binding to 14-3-3 proteins modulates keratin filaments and hepatocyte mitotic progression. Proc. Natl. Acad. Sci. USA *99,* 4373–4378.

Kulesh, D.A., and Oshima, R.G. (1988). Cloning of the human keratin 18 gene and its expression in nonepithelial mouse cells. Mol. Cell. Biol. *8,* 1540–1550.

Leube, R.E., Wiedenmann, B., and Franke, W.W. (1989). Topogenesis and sorting of synaptophysin: synthesis of a synaptic vesicle protein from a gene transfected into nonneuroendocrine cells. Cell *59,* 433–446.

Liao, J., and Omary, M.B. (1996). 14-3-3 proteins associate with phosphorylated simple epithelial keratins during cell cycle progression and act as a solubility cofactor. J. Cell Biol. *133,* 345–357.

Liovic, M., Mogensen, M.M., Prescott, A.R., and Lane, E.B. (2003). Observation of keratin particles showing fast bidirectional movement colocalized with microtubules. J. Cell Sci. *116,* 1417–1427.

Magin, T.M., Bader, B.L., Freudenmann, M., and Franke, W.W. (1990). De novo formation of cytokeratin filaments in calf lens cells and cytoplasts after transfection with cDNAs or microinjection with mRNAs encoding human cytokeratins. Eur. J. Cell Biol. *53,* 333–348.

Martys, J.L., Ho, C.L., Liem, R.K., and Gundersen, G.G. (1999). Intermediate filaments in motion: observations of intermediate filaments in cells using green fluorescent protein-vimentin. Mol. Biol. Cell *10,* 1289–1295.

Miller, R.K., Khuon, S., and Goldman, R.D. (1993). Dynamics of keratin assembly: exogenous type I keratin rapidly associates with type II keratin in vivo. J. Cell Biol. *122,* 123–135.

Miller, R.K., Vikstrom, K., and Goldman, R.D. (1991). Keratin incorporation into intermediate filament networks is a rapid process. J. Cell Biol. *113,* 843–855.

Ngai, J., Coleman, T.R., and Lazarides, E. (1990). Localization of newly synthesized vimentin subunits reveals a novel mechanism of intermediate filament assembly. Cell *60,* 415–427.

Omary, M.B., Ku, N.O., Liao, J., and Price, D. (1998). Keratin modifications and solubility properties in epithelial cells and in vitro. Subcell. Biochem. *31,* 105–140.

Parry, D.A., and Steinert, P.M. (1999). Intermediate filaments: molecular architecture, assembly, dynamics and polymorphism. Q. Rev. Biophys. *32,* 99–187.

Prahlad, V., Yoon, M., Moir, R.D., Vale, R.D., and Goldman, R.D. (1998). Rapid movements of vimentin on microtubule tracks: kinesin-dependent assembly of intermediate filament networks. J. Cell Biol. *143,* 159–170.

Raats, J.M., Pieper, F.R., Vree Egberts, W.T., Verrijp, K.N., Ramaekers, F.C., and Bloemendal, H. (1990). Assembly of amino-terminally deleted desmin in vimentin-free cells. J. Cell Biol. *111,* 1971–1985.

Reichenzeller, M., Burzlaff, A., Lichter, P., and Herrmann, H. (2000). In vivo observation of a nuclear channel-like system: evidence for a distinct interchromosomal domain compartment in interphase cells. J. Struct. Biol. *129,* 175–185.

Roy, S., Coffee, P., Smith, G., Liem, R.K., Brady, S.T., and Black, M.M. (2000). Neurofilaments are transported rapidly but intermittently in axons: implications for slow axonal transport. J. Neurosci. *20,* 6849–6861.

Sarria, A.J., Nordeen, S.K., and Evans, R.M. (1990). Regulated expression of vimentin cDNA in cells in the presence and absence of a preexisting vimentin filament network. J. Cell Biol. *111,* 553–565.

Small, J.V., Stradal, T., Vignal, E., and Rottner, K. (2002). The lamellipodium: where motility begins. Trends Cell Biol. *12,* 112–120.

Strelkov, S.V., Herrmann, H., and Aebi, U. (2003). Molecular architecture of intermediate filaments. Bioessays *25,* 243–251.

Strnad, P., Windoffer, R., and Leube, R.E. (2001). In vivo detection of cytokeratin filament network breakdown in cells treated with the phosphatase inhibitor okadaic acid. Cell Tissue Res. *306,* 277–293.

Strnad, P., Windoffer, R., and Leube, R.E. (2002). Induction of rapid and reversible cytokeratin filament network remodeling by inhibition of tyrosine phosphatases. J. Cell Sci. *115,* 4133–4148.

Strnad, P., Windoffer, R., and Leube, R.E. (2003). Light-induced resistance of the keratin network to the filament-disrupting tyrosine phosphatase inhibitor orthovanadate. J. Invest. Dermatol. *120,* 198–203.

Theriot, J.A. (1997). Accelerating on a treadmill: ADF/cofilin promotes rapid actin filament turnover in the dynamic cytoskeleton. J. Cell Biol. *136,* 1165–1168.

Troyanovsky, S.M., Eshkind, L.G., Troyanovsky, R.B., Leube, R.E., and Franke, W.W. (1993). Contributions of cytoplasmic domains of desmosomal cadherins to desmosome assembly and intermediate filament anchorage. Cell *72,* 561–574.

Vaezi, A., Bauer, C., Vasioukhin, V., and Fuchs, E. (2002). Actin cable dynamics and Rho/Rock orchestrate a polarized cytoskeletal architecture in the early steps of assembling a stratified epithelium. Dev. Cell *3,* 367–381.

Vikstrom, K.L., Borisy, G.G., and Goldman, R.D. (1989). Dynamic aspects of intermediate filament networks in BHK-21 cells. Proc. Natl. Acad. Sci. USA *86,* 549–553.

Vikstrom, K.L., Lim, S.S., Goldman, R.D., and Borisy, G.G. (1992). Steady state dynamics of intermediate filament networks. J. Cell Biol. *118,* 121–129.

Wang, L., and Brown, A. (2001). Rapid intermittent movement of axonal neurofilaments observed by fluorescence photobleaching. Mol. Biol. Cell *12,* 3257–3267.

Wang, L., Ho, C.L., Sun, D., Liem, R.K., and Brown, A. (2000). Rapid movement of axonal neurofilaments interrupted by prolonged pauses. Nat. Cell Biol *2,* 137–141.

Weber, K.L., and Bement, W.M. (2002). F-actin serves as a template for cytokeratin organization in cell free extracts. J. Cell Sci. *115,* 1373–1382.

Werner, N.S., Windoffer, R., Strnad, P., Grund, C., Leube, R.E., and Magin, T.M. (2004). *Epidermolysis bullosa simplex*-type mutations alter the dynamics of the keratin cytoskeleton and reveal a contribution of actin to the transport of keratin subunits. Mol. Biol. Cell *15,* 900–1002.

Windoffer, R., Borchert-Stuhltrager, M., and Leube, R.E. (2002). Desmosomes: interconnected calcium-dependent structures of remarkable stability with significant integral membrane protein turnover. J. Cell Sci. *115,* 1717–1732.

Windoffer, R., and Leube, R.E. (1999). Detection of cytokeratin dynamics by time-lapse fluorescence microscopy in living cells. J. Cell Sci. *112,* 4521–4534.

Windoffer, R., and Leube, R.E. (2001). De novo formation of cytokeratin filament networks originates from the cell cortex in A-431 cells. Cell Motil. Cytoskel. *50,* 33–44.

Yoon, K.H., Yoon, M., Moir, R.D., Khuon, S., Flitney, F.W., and Goldman, R.D. (2001). Insights into the dynamic properties of keratin intermediate filaments in living epithelial cells. J. Cell Biol. *153,* 503–516.

Yoon, M., Moir, R.D., Prahlad, V., and Goldman, R.D. (1998). Motile properties of vimentin intermediate filament networks in living cells. J. Cell Biol. *143,* 147–157.